Nanosecond control and optical pulse shaping by stimulated emission depletion in a liquid crystal

Maruša Vitek[1] **and Igor Muševič**[1,2,*]

[1]*J. Stefan Institute, Jamova 39, SI-1000, Ljubljana, Slovenia*
[2]*Faculty of Mathematics and Physics, University of Ljubljana, Jadranska 19, SI-1000, Ljubljana, Slovenia*

[*]*igor.musevic@ijs.si*

http://www.softmatter.si/

Abstract: We study anisotropic Stimulated Emission Depletion (STED) from dye molecules, which are collectively ordered in a host liquid crystal. Due to the ordering of fluorescent emitters, the STED efficiency depends on the polarization of the depletion beam and time-delay of the STED pulse. The depletion efficiency is highest at lower temperatures in the highly ordered smectic-A phase and deteriorates in the higher temperature nematic and isotropic phases. We demonstrate by temporal tuning of STED that it is possible to generate an arbitrary sequence of nanosecond fluorescent pulses with variable width and variable delay. Our results show that the STED mechanism in principle allows for very fast (GHz) and efficient control of light by light, which could in the future be used for all-optical control of the flow of light in photonic microdevices based on liquid crystals. Using STED anisotropy and time-control, new modalities of STED imaging in liquid crystals could be developed.

OCIS codes: (230.3720) Liquid-crystal devices; (160.1190) Anisotropic optical materials; (160.2540) Fluorescent and luminescent materials.

References and links

1. S. W. Hell and J. Wichman,"Breaking the diffraction resolution limit by stimulated emission: stimulated-emission-depletion fluorescence microscopy," Opt. Lett. **19**, 780–782 (1994).
2. I. Gryczynski, J. Kusba, and J. R. Lakowicz,"Light quenching of fluorescence using time-delayed laser pulses as observed by frequency-domain fluorometry," J. Phys. Chem. **98**, 8886–8895 (1994).
3. J. R. Lakowicz, I. Gryczynski, V. Bogdanov, and J. Kusba,"Light quenching and fluorescence depolarization of Rhodamine B and applications of this phenomenon to biophysics," J. Phys. Chem. **98**, 334–342 (1994).
4. J. Kusba, V. Bogdanov, I. Gryczynski, and J. R. Lakowicz,"Theory of light quenching: effects on fluorescence polarization, intensity, and anisotropy decays," Biophys. J. **67**, 2024–2040 (1994).
5. T. A. Klar and S. W. Hell, "Subdiffraction resolution in far-field fluorescence microscopy," Opt. Lett. **24**, 954–956 (1999).
6. T. A. Klar, S. Jakobs, M. Dyba, A. Egner, and S. W. Hell, "Fluorescence microscopy with diffraction resolution barrier broken by stimulated emission," Proc. Natl. Acad. Sci. USA **97**, 8206–8210 (2000).
7. D. Wildanger, E. Rittweger, L. Kastrup, and S. W. Hell, "STED microscopy with a supercontinuum laser source," Opt. Express **16**, 9614–9621 (2008).
8. J. Bückers, D. Wildanger, G. Vicidomini, L. Kastrup, and S. W. Hell, "Simultaneous multi-lifetime multi-color STED imaging for colocalization analyses," Opt. Express **19**, 3130–3143 (2011).

#236079 Received 12 Mar 2015; revised 22 May 2015; accepted 28 May 2015; published 19 Jun 2015

9. B. Bahadur, "Guest-host effect," in *Handbook of Liquid Crystals Vol. 2A*, D. Demus, J. Goodby, G. W. Gray, H. W. Spiess, and V. Vill, eds., (Wiley-VCH Verlag GmbH Weinheim, 1998), pp. 257–302
10. C. Zannoni, "A theory of time dependent fluorescence depolarization in liquid crystals," Mol. Phys. **38**, 1813–1827 (1979).
11. R. Arcioni, F. Bertinelli, R. Tarroni, and C. Zannoni,"Time resolved depolarization fluorescence in a nematic liquid crystal," Mol. Phys. **61**, 1161–1181 (1987).
12. I. I. Smalyukh, S. V. Shyanovskii, and O. D. Lavrentovich,"Three-dimensional imaging of orientational order by fluorescence confocal microscopy," Chem. Phys. Lett. **336**, 88–96 (2001).
13. M. Humar, M. Ravnik, S. Pajk, and I. Muševič, "Electrically tunable liquid crystal optical microresonators," Nat. Photonics **3**, 595–600 (2009).
14. M. Humar and I. Muševič, "3D microlasers from self-assembled cholesteric liquid-crystal microdroplets," Opt. Express **18**, 26995–27003 (2010).
15. D. J. Gardiner, S. M. Morris, P. J. W. Hands, C. Mowatt, R. Rutledge, T. D. Wilkinson, and H. J. Coles, "Paintable band-edge liquid crystal lasers," Opt. Express **19**, 2432–2439 (2011).
16. G. Cipparrone, A. Mazzulla, A. Pane, R. J. Hernandez, and R. Bartolino, "Chiral self-assembled solid microspheres: A novel multifunctional microphotonic device," Adv. Mat. **23**, 5773–5778 (2011).
17. M. Humar and I. Muševič, "Surfactant sensing based on whispering-gallery-mode lasing in liquid-crystal microdroplets," Opt. Express **19**, 19836–19844 (2011).
18. K. Peddireddy, P. Kumar, S. Thutupalli, S. Herminghaus, and Ch. Bahr, "Solubilization of thermotropic liquid crystal compounds in aqueous surfactant solutions," Langmuir **28**, 12426–12431 (2012).
19. K. Peddireddy, V. S. R. Jampani, S. Thutupalli, S. Herminghaus, Ch. Bahr, and I. Muševič,"Lasing and waveguiding in smectic A liquid crystal optical fibers," Opt. Express **21**, 30233–30242 (2013)
20. V. S. R. Jampani, M. Humar, and I. Muševič, "Resonant transport of light from planar polymer waveguide into liquid-crystal microcavity," Opt. Express **21**, 20506–20516 (2013).
21. E. Brasselet, N. Murazawa, H. Misawa, and S. Joudkazis, "Optical vortices from liquid crystal droplets," Phys. Rev. Lett. **103**, 103903 (2009).
22. G. Tkachenko and E. Brasselet, "Helicity-dependent three-dimensional optical trapping of chiral microparticles," Nature Comm. **5**, 4491 (2014).
23. R. J. Hernandez, A. Mazzulla, A. Pane, K. Volke-Sepulveda, and G. Cipparrone, "Attractive-repulsive dynamics on light-responsive chiral microparticles induced by polarized tweezers," Lab on a Chip **13** 459–467 (2013).
24. I. Muševič, "Nematic colloids, topology and photonics," Phil. Trans. Royal Soc. A **371**, 20120266 (2013).
25. I. Muševič, "Integrated and topological liquid crystal photonics," Liquid Crystals **41**, 418–429 (2014).
26. H. Tajalli, A. Ghanadzadeh Gilani, M. S. Zakerhamidi, and P. Tajalli, "The photophysical properties of Nile red and Nile blue in ordered anisotropic media," Dyes and Pigments **78**, 15–24 (2008).
27. M. Choi, D. Jin, H. Kim, "Fluorescence anisotropy of Nile red and Oxazine 725 in an isotropic liquid crystal," J. Phys. Chem. B **101**, 8092–8097 (1997).
28. M. Vilfan, T. Apih, P. J. Sebastião, G. Lahajnar, and S. Žumer, "Liquid crystal 8CB in random porous glass: NMR relaxometry study of molecular diffusion and director fluctuations," Phys. Rev. E **76**, 051708 (2007).
29. F. M. Aliev, Z. Nazario, and G. P. Sinha, "Broadband dielectric spectroscopy of confined liquid crystals," J. Non-Cryst. Solids **305**, 218–225 (2002).
30. T. Scheul, C. D'Amico, I. Wang, and J.-C. Vial,"Two-photon excitation and stimulated emission depletion by a single wavelength," Opt. Express **19**, 18036–18048 (2011).
31. A. J. Bain, R. J. Marsh, D. A. Armoogum, O. Mongin, L. Porres, and M. Blanchard-Desce,"Time-resolved stimulated emission depletion in two-photon excited states," Biochemical Soc. Trans. **31**, 1047–1051 (2003).

1. Introduction

Stimulated Emission Depletion of fluorescence (STED) was first studied in 1994 by two independent groups in two different contexts. S. W. Hell and J. Wichmann considered STED as a method to bypass the diffraction limit of optical microscopes [1]. On the other hand, the group of J. R. Lakowitz considered the STED (or light quenching in their terms) as a way to modulate fluorescently emitted light on a very fast time-scale for applications in fluorometry [2–4]. Later on, Hell et al. have shown that STED microscope can bypass Abbe's diffraction limit for fluorescently labeled samples by an order of magnitude [5, 6] by using a combination of two beams and by collecting the fluorescence emission from the sample in reflection. Each pixel of the sample is first illuminated by a very short ($\sim$ 100 ps) excitation pulse, which is immediately followed by a second depletion pulse, with a time-delay precisely tuned to strongly deplete the spontaneous fluorescence. Whereas the excitation pulse instantaneously excites the fluorophore molecules into the excited electronic states, the depletion pulse is in resonance with the elec-

#236079 Received 12 Mar 2015; revised 22 May 2015; accepted 28 May 2015; published 19 Jun 2015

tronic transition and brings the electrons back into the ground states by stimulated emission, before the spontaneous emission could take place. The photons produced by stimulated emission are identical to the resonant photons that caused the transition, so they travel in the same direction. Therefore the stimulated emission will not be detected by the microscope's detection system in the reflected light. The depletion (or quenching) of the fluorescence emission is combined with different cross-sections of the excitation and depletion beams. Whereas the excitation beam has a Gaussian profile, the depletion beam has a doughnut-like intensity profile of the Laguerre-Gaussian type [7,8]. The geometric centers of both beams are perfectly aligned with each other, which in combination with depletion mechanism results in a spontaneous fluorescence only from the tiny and dark center of the depletion beam, where the fluorescence was not depleted. STED microscope therefore uses the principle of the photonic control of fluorescence emission and can be considered as a way of controlling the light by light in a fluorescent medium.

In liquid crystals (LCs), there is a long history of studies of fluorescence emission from dyes, which are dissolved in different liquid crystalline phases, interesting for applications in guest-host LC displays [9]. From more fundamental aspects, depolarization of fluorescence emission can give information on the dynamics and order parameter in liquid crystals [10, 11], because the dye molecules usually align along the direction of overall orientational order. Fluorescent dyes, dissolved in LCs and ordered along the LC molecules have extensively been used in Fluorescence Confocal Polarizing Microscopy (FCPM) [12].

In an entirely different research area, it was demonstrated in the last five years, that dispersions of liquid crystals in immiscible fluids, such as water, glycerine and different polymers, result in the formation of small, tens-of-micrometer diameter droplets and even micrometer-diameter fibers, which show some spectacular photonic properties. Micro-droplets of nematic liquid crystals were demonstrated to support Whispering Gallery Modes and the eigenfrequencies of these microcavities can be tuned by an electric field [13]. Because of softness of liquid crystals, tunability of WGMs is nearly two orders of magnitude higher compared to solid microresonators. Cholesteric liquid crystal microdroplets, doped with fluorescent dyes, are self-assembled 3D microlasers that emit the laser light in all directions uniformly [14–16]. When liquid crystal droplets are freely floating in liquid environment, they can be used as micro-sensors, because the WGM lasing from these droplets is surface-sensitive [17]. It was demonstrated recently that smectic-A liquid crystals can spontaneously form microfibers [18], which show excellent waveguiding and spectacular lasing properties [19]. Further on, the resonant light transport between different liquid-crystal-based microphotonic devices in close contact was demonstrated [20]. Self-assembled liquid crystal droplets and fibers not only show a variety of spectacular photonic properties, but also have interesting topological properties. Because of softness, long range order and confinement, liquid crystal droplets exhibit a variety of topological defects, or order singularities, which have a strong influence on their optical properties. This includes generation of Laguere-Gaussian beams with phase singularities [21], chiral selectivity [22] and unusual laser trapping with circularly polarized light [23]. Rapid development and some spectacular results showcasing the photonic properties of liquid crystals led to the idea of self-assembling the photonic integrated circuits entirely of soft matter [24,25]. While most of the basic problems of self-assembling, binding of microphotonic elements and light transport in LC-based microphotonic devices have in principle been solved, it remains to find out how to control in such structures the flow of light by light.

Here we propose to use stimulated emission depletion mechanism in fluorescently labeled liquid crystal elements as a way to control the light by light at a nanosecond time scale in liquid crystals. Because the liquid crystalline phases can align fluorescent emitters along the overall orientation of the LC molecules, STED should also be anisotropic and polarization dependent.

#236079 Received 12 Mar 2015; revised 22 May 2015; accepted 28 May 2015; published 19 Jun 2015

In combination with sub-nanosecond nature of STED, this could result in interesting polarization dependent all-optical control of light in liquid crystal photonic devices with nanosecond time resolution. To this aim, we study the anisotropy of fluorescence emission, as well as efficiency and temporal-control of the fluorescence emission by using the time-resolved STED mechanism in the smectic-A, nematic and isotropic phases of a liquid crystal in a thin, homogeneously aligned cell. We demonstrate that by tuning the time-delay of the STED pulses in the LC, one could generate series of optical pulses as short as one nanosecond, which together with the observed strong anisotropy of the polarization properties of STED in LC phases shows a huge potential for developing and engineering LC-based all-optical microphotonic devices based entirely on soft matter and operating at GHz rates.

2. Experiments

To study stimulated emission depletion in liquid crystals, we have built an optical setup similar to the STED microscope described in [7], and shown in Fig. 1. We are using a pulsed supercontinuum laser (Fianium SC-450-PP-HE, pulse width 150 ps, repetition 1MHz) that emits unpolarized white laser light with a continuous spectrum ranging from blue to infrared. We split the laser beam into two beams of perpendicular linear polarizations with a polarizing beam splitter (PBS). We select bands of appropriate wavelengths for each of these beams. In one beam we use a 20 nm wavelength band, centered at 532 nm, to excite the fluorescence in our sample. In the other we choose a 20 nm wavelength band centered at 705 nm, to induce strong reduction of fluorescence via stimulated emission.

After choosing the appropriate wavelengths, each beam is coupled into polarization maintaining single mode optical fibers to get rid of the higher optical modes. After being collimated out of the fibers the two beams are combined with a dichroic mirror that reflects the wavelengths under 638 nm and the beams are carefully aligned with respect to each other. They are sent into an inverted microscope (Nikon Eclipse Ti) through a back port and reflected into the optical path by a carefully selected double edge dichroic mirror that reflects wavelengths shorter than 560 nm and longer than 650 nm. The beams are focused on a sample by a microscope water immersion objective (60X, NA=1). The fluorescence is collected with the same objective. The emitted light passes through the double edge dichroic mirror and a bandpass filter and is sent either to camera, avalanche photodiode or to the spectrophotometer through an optical fiber. For imaging purposes we use a CCD camera (Canon EOS 550D). Fluorescence intensity and spectra are measured with a spectrometer (Shamrock SR-500i, Andor) equipped with a cooled EM-CCD camera (Newton DU970N, Andor). Time-resolved measurements are performed with an avalanche photodiode (APD 210, MenloSystems GmbH). The pulses are monitored and stored on a fast oscilloscope (Infiniium MSO9404A, Agilent Technologies, Inc.) with 250 ps time resolution.

We study the STED in 12 μm thick glass cells filled with 8CB (4'-octyl-4-cyanobiphenyl, Frinton Laboratories, Inc.). This material exhibits a smectic-A phase at room temperature, it changes to the nematic (N) phase at 33 °C, and becomes isotropic at 40 °C. In the nematic phase, the rod-like molecules of 8CB are spontaneously aligned into a common direction, called the director, $\boldsymbol{n}$. The molecules are positionally disordered. By lowering the temperature, the nematic phase of 8CB spontaneously transforms into the smectic-A phase. This phase preserves the spontaneous orientational order, but the LC molecules are in addition positionally ordered into molecular layers, called smectic layers, which are perpendicular to the director $\boldsymbol{n}$.

The liquid crystal is doped with a fluorescent dye Nile Red, whose molecules align parallel to the LC molecules [19]. The radiative dipole moment of Nile Red is oriented along the long axis of the dye molecules and therefore along the long axis of the 8CB molecules [26]. We impose planar anchoring on the glass surfaces inside the cell by using standard LC alignment

#236079 Received 12 Mar 2015; revised 22 May 2015; accepted 28 May 2015; published 19 Jun 2015

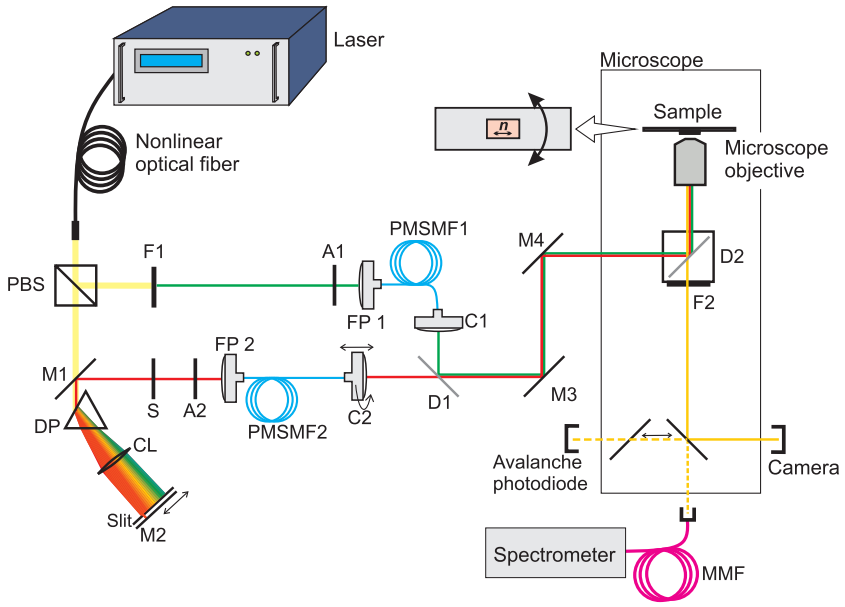

Fig. 1. Setup for the STED experiment. White light from the laser is split into two beams of perpendicular polarizations by a polarizing beam-splitter (PBS). For the excitation beam (green) we choose the wavelength band with a bandpass filter (F1). The beam passes through a continuous neutral density attenuator (A1) and is coupled into a polarization-maintaining single mode optical fiber (PMSMF1). The light is collimated at the fiber output. The STED beam wavelength (red) is chosen by a dispersing-prism-based wavelength selector by simply changing position of the slit. This beam also passes through a continuous attenuator (A2) and is coupled into the polarization-maintaining single mode fiber (PMSMF2) to be cleaned of higher optical modes. Collimator C2 is mounted so that it can be translated along the optical axis and rotated around it. This enables the change of the optical path and the rotation of the STED beam polarization. After collimation at fiber outputs, both beams are joint by a dichroic mirror (D1) that reflects wavelengths shorter than 638 nm. The beams are carefully aligned and sent into the microscope through its back port. They are both reflected to the sample on a double edge dichroic mirror (D2) and focused through a 60x water immersion objective. Fluorescence (yellow) is transmitted through the double edge dichroic mirror (D2) and a bandpass filter (F2) and sent to one of the detectors. M1, M2, M3, M4: mirrors, DP: dispersive prism, CL: cylindrical lens, S: shutter, FP1, FP2: fiber ports, MMF: multi-mode fiber.

technique of rubbing the polyimide layer (PI-2555, NISSAN Chemicals) on the glass surface with a velvet cloth in a preferred direction. This aligns both the LC and dye molecules in a given direction parallel to the glass plates throughout the cell.

3. Results and discussion

We first study the angular dependence of fluorescence intensity on the direction of the excitation beam polarization. In the experiment the excitation beam which illuminates the sample has a fixed polarization. The intensity of fluorescent emission, measured while rotating the liquid crystal cell with Nile Red doped 8CB, is shown in Fig. 2.

As expected and shown before [26, 27], Nile Red absorption and emission are strongly anisotropic and depend on the polarization of the excitation beam. The ratio of emission inten-

#236079 Received 12 Mar 2015; revised 22 May 2015; accepted 28 May 2015; published 19 Jun 2015

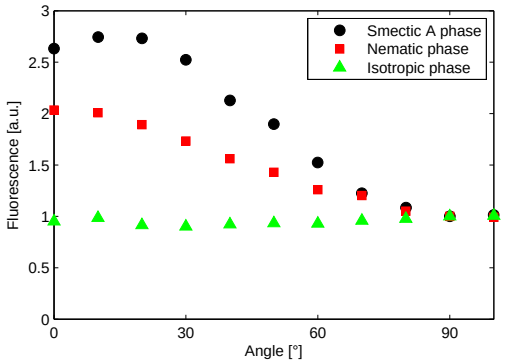

Fig. 2. Angular dependence of fluorescence in 8CB/Nile Red mixture. For each LC phase the fluorescence signal is divided by its value at 90° and presented in dependence of the angle between the excitation beam polarization and the director. In smectic-A phase the ratio between intensities at parallel (0°) and perpendicular (90°) arrangements is around 3, in nematic phase around 2 and in isotropic phase fluorescence intensity is independent of the angle between excitation beam polarization and the director.

sities for parallel (0°) and perpendicular (90°) arrangements is highest in the smectic-A phase (around 3), it is lower in the nematic phase (around 2) and equal to 1 in the isotropic phase, as expected. Namely, this anisotropy is proportional to the degree of the molecular ordering (or the order parameter), which is highest in the highly ordered smectic-A phase and decreases to zero in the isotropic phase.

In the next experiment, we include the STED beam with polarization set parallel to the polarization of the excitation beam and the director. By making sure that both beams are well aligned and overlapping before they enter the microscope, and that the optical paths of both beams are of the same length, we immediately observe the STED effect. When the shutter in the STED beam is closed, we can see a bright spot of fluorescence emission from the illuminated spot on the sample. By opening the STED beam we can clearly see the darkening of that spot. When the optical path and wavelength of the STED beam are optimized we can observe huge decrease in fluorescence intensity, as shown in Fig. 3.

The optimal central wavelength for the STED beam is determined by using a wavelength selector, based on a dispersing prism and a movable slit. By changing the position of the slit we can select a certain wavelength band out of the dispersed supercontinuum white light. By measuring the intensity of depleted fluorescence from the sample we determine the optimal STED wavelength, where the STED beam is most efficient. For our sample this is around 705 nm (Fig. 4(a)).

In addition to choosing the optimum STED wavelength, we need to optimize the STED efficiency by fine-tuning the time-delay between the excitation and STED pulse arrivals. To this aim, we mount the STED output collimator (C2, see Fig. 1) on rails, which enables us to vary the optical path of the STED beam for up to 30 cm. This results in a delay between the excitation and STED pulses in the range of $\sim$1 ns (Fig. 4(b)). When the optical path of the STED beam is decreased too much, the STED pulse arrives to the sample before the excitation pulse and therefore cannot affect the fluorescence emission. In this case we observe no fluorescence depletion. By increasing the optical path of the STED beam, these pulses start to overlap the excitation pulses and we can see diminishing of the fluorescence, which decreases by increasing the time-overlap. Finally we reach a point where the STED pulse is most effective. From the point where there was no STED effect to the point where we reached the best effectiveness we

#236079 Received 12 Mar 2015; revised 22 May 2015; accepted 28 May 2015; published 19 Jun 2015

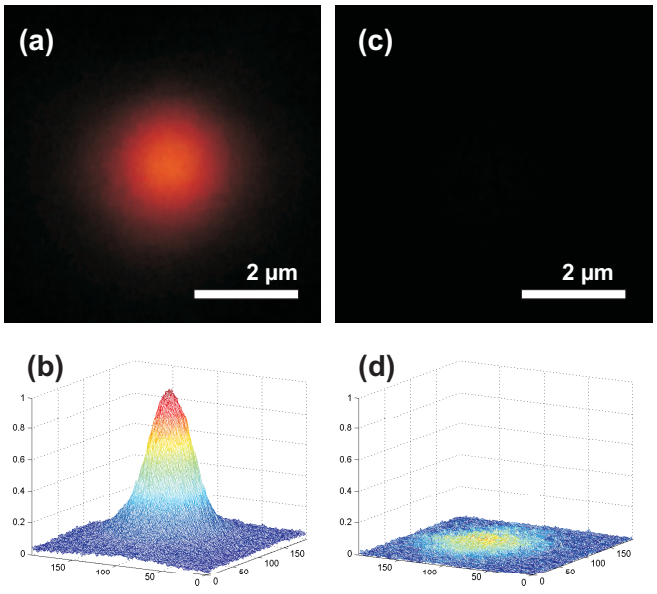

Fig. 3. Microscope images and fluorescence intensity profiles of the illuminated area of the 8CB/Nile Red mixture. Both polarizations of the excitation and STED beam are parallel to the director. (a), (b) Only the excitation beam (532 nm) is illuminating the sample, with polarization along the director (and the radiative dipole of Nile Red), which results in the observed fluorescence emission. (c), (d) The STED beam (705 nm), polarized along the director is switched on, which causes a strong decrease of fluorescence emission.

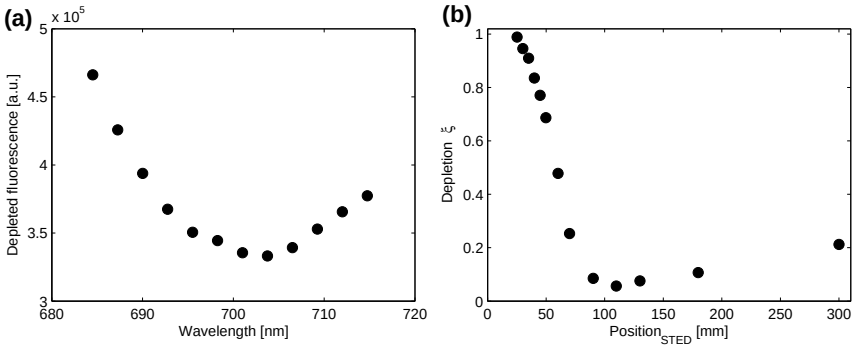

Fig. 4. Optimization of the STED beam wavelength and pulse delay. The polarizations of the STED and excitation beams are parallel to the director. (a) For Nile Red dye in 8CB, the STED effect is strongest if we use 705 nm wavelength for the STED beam. (b) Depletion of the fluorescence caused by the STED beam depends on the time-delay between the excitation and the STED pulse and is strongest at the coupler position, which corresponds to approximately 150 ps delay. The depletion "ξ" denotes the ratio of depleted and non-depleted intensities.

increased the optical path for approximately 10 cm which corresponds to $\sim$300 ps. By increasing the delay between the pulses to $\sim$1 ns we can observe a decrease of the STED efficiency. This is due to the fact, that here the delay between the pulses becomes comparable to the flu-

#236079 Received 12 Mar 2015; revised 22 May 2015; accepted 28 May 2015; published 19 Jun 2015

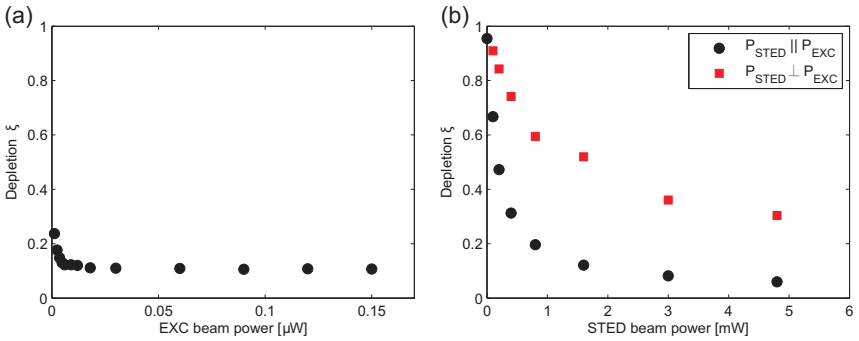

Fig. 5. Dependence of the STED depletion on the excitation and STED beam average power. The polarizations of the STED and excitation beams are parallel to the director. (a) STED depletion is measured at constant STED beam intensity and the excitation power is increased. Depletion is poor at low excitation beam power, because the fluorescence intensity here becomes comparable to fluorescence intensity caused by the STED beam itself. (b) We show measurement of STED depletion at constant excitation beam power when the STED beam power increases. Two measurements are presented, one (black circles) for the case when the STED beam polarization is parallel to the excitation beam polarization and the director field and the other (red squares) for the case when it is perpendicular.

orescence lifetime (ns range). In this case the STED pulse arrives after a considerable amount of molecules have already had relaxed by spontaneous emission and the depletion therefore is inefficient.

The STED effect depends on the STED beam intensity as well as on the excitation beam intensity. Figure 5(a) shows the measurement of depletion ξ, the ratio of depleted and non-depleted fluorescence intensity, when the STED beam intensity is kept constant (3 mW) and the excitation beam intensity is increased. For simplicity we show depletion ξ in dependence of the average beam power measured at the back port of the microscope. Although the STED beam wavelength is selected on the red edge of the fluorescence spectrum, it still causes a small fluorescence signal. For this reason, the STED efficiency is low (i.e. the depleted intensity is relatively high), when the excitation beam is weak. However, very soon the curve becomes flat and the STED efficiency is independent on the excitation power. On the other hand, rather high excitation beam power causes photo-bleaching of the sample, which should be avoided. The optimal excitation beam power is around 0.03 μW, where the STED efficiency reaches the plateau. The STED beam in this case causes a decrease of the fluorescence signal by the factor 10 ($\xi \sim 0.1$). Figure 5(b) shows the dependence of the depletion on the STED beam average power. In this case the excitation beam intensity is kept constant (0.03 μW) and the STED beam intensity is increased. Here, the depletion gradually increases with increasing the STED beam power, the optimum is at the highest reachable STED beam power (in our case $\sim$ 5 mW). By considering the laser repetition rate (1 MHz), length of laser pulses (150 ps) and the estimated STED beam waist diameter in the focus (1.5 μm) we see that 5 mW of average power corresponds to the power density > 1 GW/cm^2 on the sample. Comparison of Figs. 5(a) and 5(b) clearly shows that the optimal ratio between the power of the excitation and STED beam is $\sim 10^5 : 1$.

Because the fluorescent emitters are well aligned along the average direction of LC molecules, the STED effect should be angularly dependent, and the STED depletion should be strongest for the STED polarization along the radiative dipole moment of Nile Red molecules.

#236079 Received 12 Mar 2015; revised 22 May 2015; accepted 28 May 2015; published 19 Jun 2015

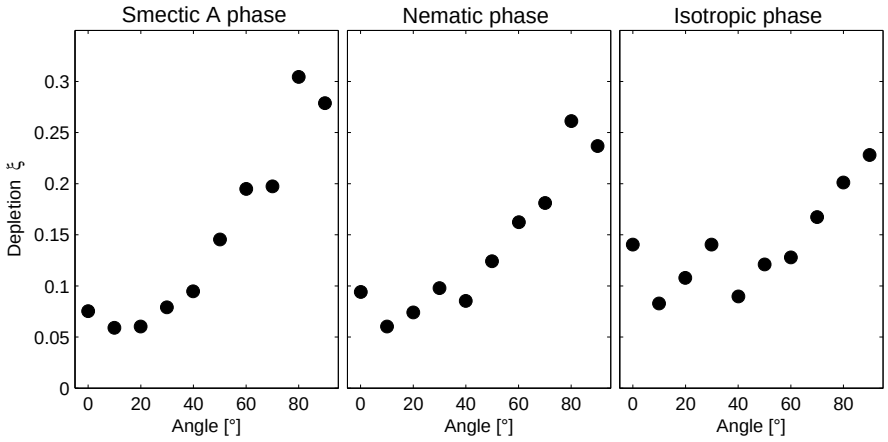

Fig. 6. The angular dependence of the STED effect in smectic-A, nematic and isotropic phase. In all cases the polarization of the excitation beam is set parallel to the director and the STED polarization is set at an angle from 0 to 90 degrees. Depletion "ξ" denotes the ratio of depleted and non-depleted intensities.

On the time-average this coincides with the overall orientation of the LC. Since we are using polarization maintaining optical fibers, we are able to control the output polarization of the STED beam by rotating the output coupler (C2) around the fiber axis. That way we can have STED beam polarization parallel, perpendicular or at an arbitrary angle to the excitation beam polarization. The polarization of the excitation beam is set parallel to the director, so that the fluorescence emission is the highest possible. We show in Fig. 6 that the STED effect is polarization dependent and the depletion is strongest, when the polarization is parallel to the director (and to the radiative dipole moment). In smectic phase the depletion efficiency between parallel and perpendicular STED polarizations is most pronounced, and it is least pronounced in the isotropic phase. This can be understood in view of the Nile Red molecular ordering and dynamics within the nematic host. Dye molecules, as well as LC molecules, exhibit strong thermal fluctuations of the orientation of their long molecular ordering, which is the reason for strong depolarized light scattering in nematic liquid crystals. In most extreme case, molecules exhibit flipping around their short molecular axes, which corresponds to molecular rotation for 180 $^\circ$. These reorientations are fast, with the relaxation rate in the nanosecond region [28, 29]. At lower temperatures, in the smectic-A phase, the orientational dynamics of the LC is slower and the Nile Red molecules do not have enough time to reorient their radiative dipole moment in a $\sim$ 100 ps time window between the excitation and STED pulse. This means that STED is most efficient for polarization parallel to the excitation polarization. With increasing temperature and increased disorder, faster reorientational dynamics allows Nile Red molecules to reorient significantly in a $\sim$ 100 ps time window. This means that the molecules have enough time to turn their radiative moment significantly, which means that STED gets less dependent on the angle between the excitation and STED beam polarizations.

The temperature dependencies of the STED effect efficiency, measured at 10 different angles of the polarization of the STED beam are shown in Fig. 7. One can see that for the STED polarization angles between 0 and 45 degrees, the STED is most effective at lower temperatures (in the smectic-A phase) and loses the efficiency at higher temperatures, i.e. in the nematic and isotropic phases. The opposite is observed when the polarization of the STED beam is between 45 and 90 degrees; in this case, the STED is less efficient in the smectic-A phase, but becomes

#236079 Received 12 Mar 2015; revised 22 May 2015; accepted 28 May 2015; published 19 Jun 2015

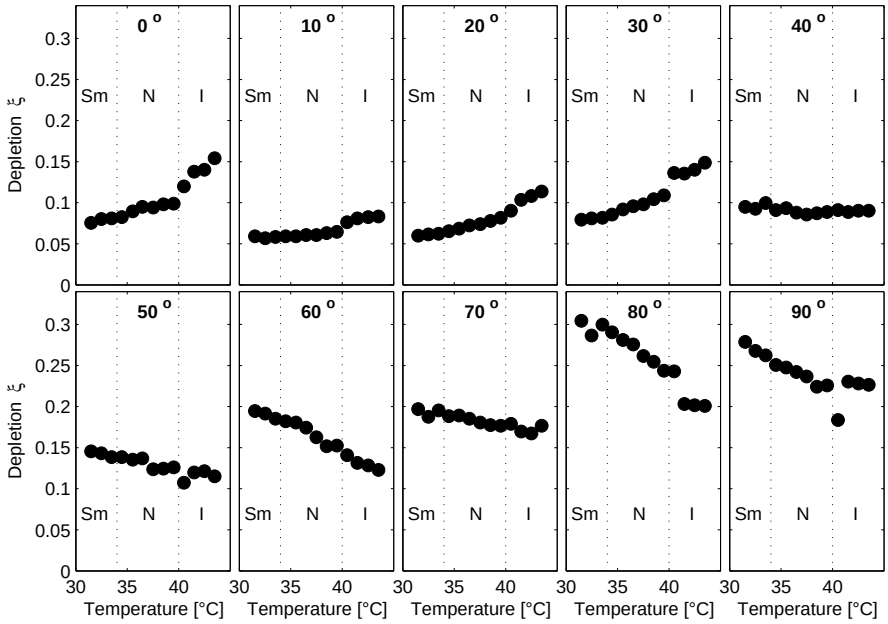

Fig. 7. Temperature dependence of the STED efficiency at 10 different angles of the polarization of the STED beam. The polarization of the excitation beam is in all measurements set parallel to the director. Depletion "ξ" denotes the ratio of depleted and non-depleted intensities.

more efficient at higher temperatures, where the LC is more disordered. This general trend can be understood in terms of dye molecular dynamics and timing of the STED pulse with respect to the excitation pulse. At small angles STED is more efficient at lower temperatures because the molecules that get excited, do not have time to reorient. The STED beam, polarized in a direction similar to their orientation, can deplete them efficiently. At higher temperatures a significant amount of excited molecules has enough time to turn before the STED beam reaches them. The depletion is therefore less efficient. The situation is opposite at higher angles. Note that the overall depletion decreases with the increasing angle.

Because the primary focus of this paper is on the polarization-sensitive control of light by light in the LCs, we are interested whether it is possible to generate and shape arbitrary sequence of optical pulses using STED in fluorescently labeled LCs. STED mechanism in principle allows for direct time-resolved control of light by light via the emitted fluorescence. If we consider spontaneous fluorescence from dye molecules, excited by a short excitation light pulse, it should in principle be possible to control the duration of the emitted fluorescence by the application of a time-delayed STED pulse. Previous time-resolved STED experiments were performed in contexts quite different from ours, such as STED imaging using two-photon excitation [30] or study of time-resolved fluorescence using STED to modify the excited electronic states [31].

To this aim, we performed time-resolved STED experiments in Nile Red labeled 8CB samples, where a temporal analysis of the emitted fluorescence was monitored under the application of a time-delayed STED pulse. The results are shown in Fig. 8, where the STED pulse is delayed by a variable time, starting from $\sim$6 ns in Fig. 8(a) to $\sim$100 ps in Fig. 8(e). One can see

#236079 Received 12 Mar 2015; revised 22 May 2015; accepted 28 May 2015; published 19 Jun 2015

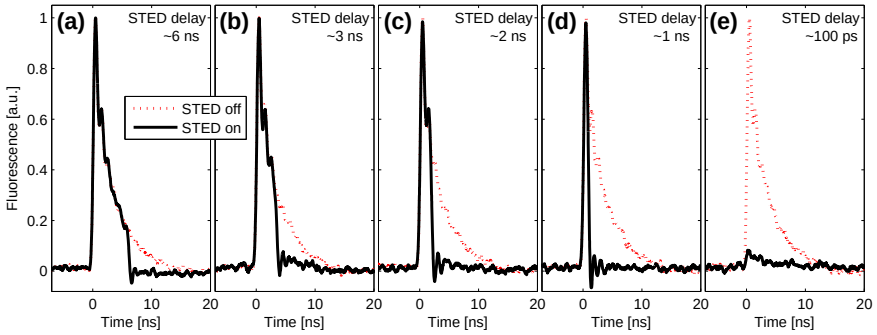

Fig. 8. Controlled shortening of the emitted fluorescence by applying a time-delayed STED pulse. In (a), the STED pulse was delayed for ∼6 ns. Note a sudden decrease of the fluorescence to zero, after a 150 ps STED pulse was applied. The delay time of the STED pulse was gradually shortened in (b)-(e), which resulted in shortening of the emitted fluorescent light. The delay time was roughly estimated from the optical path measurement with uncertainty of 50 ps. The red dotted line shows spontaneous fluorescence when no STED pulse is applied.

that indeed, the duration of the emitted fluorescent pulse can be perfectly controlled by delaying the STED pulse. Fluorescent pulses as short as ∼1 ns can easily be generated, and possibly even shorter, which however cannot be resolved in our current setup due to the limited bandwidth of the photoamplifier.

The flexibility in pulse generation and shaping was further analyzed by applying to the LC sample two consecutive 150 ps excitation pulses, where each of the pulses was followed by a time-delayed STED pulse. Here, the two consecutive excitation pulses were generated by splitting a single beam into two beams and using a variable delay line for one of these beams. At the same time, the STED beam was also split into two beams, where one of the beams was passing through a variable delay line, thus allowing for the control of the STED pulse delay.

The results are shown in Fig. 9. In Fig. 9(a), the two excitation pulses were separated by 2.9 ns, and the same separation was kept for two STED pulses, shown in Fig. 9(c). The STED pulses were delayed for 1.0 ns with respect to the excitation pulse, which resulted in two very short (∼1 ns) fluorescent pulses, separated by ∼3 ns. As one can see from Figs. 9(b) and 9(d), both the separation and width of these remaining fluorescent pulses could be arbitrarily controlled.

4. Conclusions

This work demonstrates new applications of STED mechanism in time-controlled shaping and generation of short and polarized sequences of fluorescent pulses from fluorescently labelled LC samples. Whereas in the past, the STED mechanism was primarily and successfully implemented in super-resolution scanning fluorescence imaging and fluorescence spectroscopy, little attention was given to using it as a mechanism to optically control and shape the optical pulses in photonic devices. Our work clearly demonstrates that the STED mechanism in principle allows for very fast and efficient control of light by light and this could in the future open new ways of all-optical control of the flow of light in photonic microdevices based on liquid crystals and complexly ordered soft matter in general.

Moreover, polarized STED microscopy in orientationally ordered soft matter systems could use advantages of orientationally ordered fluorescent emitters and preparation of exotic electronic states of excited dye molecules. This might lead to new STED imaging modalities in

#236079 Received 12 Mar 2015; revised 22 May 2015; accepted 28 May 2015; published 19 Jun 2015

complexly ordered soft matter, such as depolarization imaging etc.

Acknowledgments

This work was supported by the Slovenian Research Agency (ARRS) contracts PR-05543 (M.V.), P1-0099 and J1-6723 (I. M.).

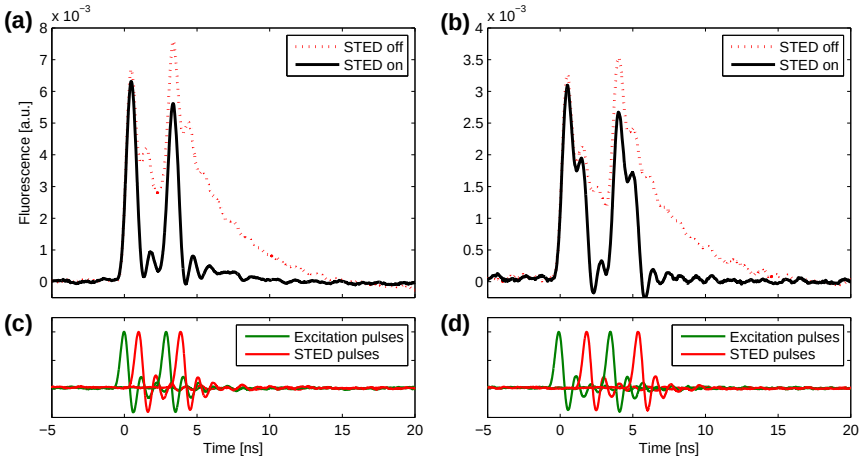

Fig. 9. Controlling the time-delay and width of two consecutive fluorescence pulses by STED. (a) Fluorescence from the Nile Red stained 8CB sample, when two 150 ps excitation pulses were applied, separated in time by 2.9 ns. Synchronously with that, two 150 ps STED pulses were applied, but each with a delay of 1.0 ns. The red dotted line shows non-depleted fluorescence emission. Time traces of the excitation and STED pulses are shown in (c). (b) The same as in (a), but in this case the delay between the excitation pulses is longer, 3.6 ns, and the delay between the excitation and STED pulse was now 1.9 ns. Note that the pulses of the emitted fluorescent light are longer compared to (a). (d) Time traces of the excitation and STED pulses for the (b) case.

#236079 Received 12 Mar 2015; revised 22 May 2015; accepted 28 May 2015; published 19 Jun 2015